

INVESTIGATION ON THE EFFECT OF PHASE CHANGING MATERIALS ON THE THERMAL PERFORMANCE OF A GREEN HOUSE USING THE FINITE VOLUME METHOD

Moghtaderi, Behdad (1); Luo, Caimao (1); Alterman, Dariusz (1); Hands, Stuart (1); Page, Adrian (1); Parks, Sophie (2); Badgery-Parker, Jeremy (2)

Organization(s): 1: University of Newcastle, Australia; 2: Division of Primary Industries, Industry & Investment NSW

ABSTRACT

The canopy wall in the greenhouse is modelled as windows in the building simulation software, so as to avoid using the concept of overall heat transfer coefficient between inside greenhouse air and outside atmosphere air in the traditional greenhouse modelling. In this greenhouse modelling software based on building simulation software, phase changing materials are considered as internal walls in the greenhouse, and the ground is modelled by 20 layers of soil. In this preliminary study, sensitivity of the ground surface solar absorption coefficient, ventilation, and geometry of the phase changing materials to the thermal performance of the greenhouse are investigated.

INTRODUCTION

The widely used energy balance equation for the green house is expressed by the following linear relationship (Kumar et al. (2010) Energy and Buildings 42 1075-1083):

$$\mu G_0 - k_s \Delta T - k_L \Delta e - K_c \Delta T - Q_m = 0 \quad (1)$$

In which G_0 is the atmosphere global solar radiation in W/m^2 , μ is the solar heating efficiency, ΔT is the temperature difference between inside and outside air temperatures, Δe is the water vapour pressure difference between the inside and outside air, K_s (in $W/(m^2K)$), K_L (in $W/(m^2Pa)$) and K_c (in $W/(m^2K)$) are the sensible, latent and overall heat transfer coefficients between inside and outside correspondingly, and Q_m is the soil heat flux (in W/m^2). It can be noted that the overall heat transfer coefficient K_c is defined with respect to the whole green house, not to a specific wall or roof, resulting in difficulty to find the K_c value for a specific greenhouse due to its dependence on greenhouse geometries.

To avoid using the concept of overall heat transfer coefficient between inside and outside air temperature, the Newcastle University Modelling and Building Energy Rating Software (NUMBERS) was modified to consider the properties of greenhouse and phase changing materials (refer to Luo et al. (2011), Luo et al. (2010a, b), Luo et al. (2008)).

To treat phase changing materials, the software should possess a capability of treating the varying

specific heat capacity and thermal conductivity. Because specific heat capacity (C_p) of PCMs is dependent on the temperature around the melting point of a PCM, analytical and response factor methods can only be used for constant ρC_p and thermal conductivity, however, finite difference or finite volume method is suitable for varying ρC_p and thermal conductivity for building materials. Heim and Clarke (2004) updated the ESP-r system by incorporating PCMs modelling via effective heat capacity method, and simulated a three-zone house with 12 mm thick of PCM-containing gypsum with a set of melting points (21, 24, 27 and 30 °C). They concluded that the effect of latent heat storage on the thermal behaviour of the building did not cause a considerable reduction in diurnal temperature fluctuation, it did decrease the internal air temperature in the seasonal transitions periods when the solar energy was effectively stored, and the numerical model needs further validation against the experimental measurements. Athienitis et al. (1997) performed an experimental and numerical simulation study in a full-scale outdoor test room with PCMs gypsum board as inside wall lining. An explicit finite difference model was developed to simulate the transient heat transfer process in the walls, and the heat of fusion was modelled as a heat source for a melting process or as a heat sink for a freezing process. It shows that utilization of the PCM gypsum board may reduce the maximum room temperature by about 4°C during the day and can reduce the heating load at night significantly. Onishi et al. (2001) numerically investigated the effects of PCMs as a heat storing material on the performance of a hybrid heating system with a CFD code. Simulated results indicated the effectiveness of PCMs and suggested the possibility of developing low-energy houses with the hybrid system introduced in this study. Using TRNSYS, Ibanez et al. (2005) evaluated the influence of walls/ceiling/floor with PCM in the whole energy balance of a building (free cooling). Bransier (1979) was the first to analyze cyclic melting/freezing of PCMs. He used a one dimensional conduction model to analyse conductive cyclic phase change of a slab and a concentric PCM module and found that a maximum of two interfaces could coexist during cyclic melting/freezing.

All of the above finite volume or finite difference methods directly used the effective specific heat

capacity model during discretizing the Fourier thermal conductivity differential equation. It can be revealed in the following section that effective specific heat capacity at any time should be obtained by the enthalpy difference by applying the energy balance equation over a control volume of the building walls, leading to that the effective specific heat capacity is dependent on its previous value and the $C_p - T$ property curve. This numerical technique has been implemented in the NUMBERS software and the preliminary results were obtained, showing the reasonable thermal performance dependence of greenhouse on PCM. However, this model still needs experimental validation in the laboratory-controlled and natural climates from the project with National Centre for Greenhouse Horticulture, NSW Department of Primary Industries.

SUBMODELS OF THE SOFTWARE

The main purpose of the software is to predict the energy consumption for greenhouse. Fundamental sub-models in the modified energy simulation program include (1) a weather model which determines the heat flux of the exterior surfaces due to short/long wave length radiations; (2) a internal wall model which presents a correlation of the heat fluxes and temperatures on both surfaces of a wall; (3) canopy model which predicts the heat transfer across the greenhouse canopy; (4) a ground model which characterises the thermal behaviour of the ground below the structure and determines the heat flux on the floor surface; (5) a zone model which establishes the energy balance equation applied to the greenhouse zone air. For the weather model, the measured solar radiation heat flux upon the horizontal and vertical planes were used to calculate the solar heat flux upon planes of other orientation.

Weather model

The purpose of the weather model is to predict: the net beam and diffuse irradiation on the outer surfaces based on the direct irradiation on a plane normal to the solar beam, the global solar irradiation and diffuse irradiation on a horizontal surface; and the convective heat transfer coefficient based on the geometry of the building and the wind speed and direction. The net heat flux on the outer surface of a wall reads

$$q_{ow} = \alpha_s (I_{sb} + I_{sd}) + \varepsilon_2 \sigma (T_2^4 - T_{sky}^4) + H_1 (T_2 - T_a) \quad (2)$$

In which q_{ow} is the net heat flux, α_s is the solar absorptance, ε_2 is the emissivity, H_1 is the convective heat transfer coefficient, I_{sb} and I_{sd} are the beam and diffusive solar irradiation on the surface, T_2 , T_a and T_{sky} are the outer surface temperature, outside air temperature and the sky temperature respectively.

The beam solar irradiation is given by:

$$I_{sb} = (I_{hG} - I_{hd}) \cos \theta / \sin \alpha \quad (3)$$

Several models are available for users to choose for calculating the diffuse solar irradiation with the default model by Hay and Davies (1980):

$$\frac{I_{sd}}{I_{hd}} = [(I_{hG} - I_{hd}) / I_E] (\cos \theta / \sin \theta_Z) + [1 - (I_{hG} - I_{hd}) / I_E] \left(\cos^2 \frac{\Sigma}{2} \right) \quad (4)$$

The convective heat transfer coefficient can be determined from several models also with the default model by Jayamaha et al. (1996):

$$H_1 = 4.955 + 1.444 V_w \quad (5)$$

Wall energy balance equations with varying thermal capacitance

The key differences for existing building thermal performance software come from the way to treat the solid walls. The Fourier diffusion equation for a solid wall is

$$\rho C_p \frac{\partial T}{\partial t} = k \frac{\partial^2 T}{\partial x^2} \quad (6)$$

in which ρ denotes density, C_p is the specific capacity, k is the thermal conductivity of the layer, T is the temperature across the layer, t is the time and x is the distance across the layer. A new finite volume scheme and a hybrid finite volume- finite difference are introduced below for discretizing the partial differential equation (6).

The pure material in any building walls is selected as the fundamental element which is divided uniformly into three computational elements with a spatial step of Δx , and temperatures at the four computational nodes (from outside to inside) are T_{s0} , T_1 , T_2 and T_{cs1} as shown in Figure 1. The surface heat fluxes at outer and inner surfaces are q''_{s0} and q''_{cs1} respectively. The length of the pure material is $L_t = 3 \Delta x$.

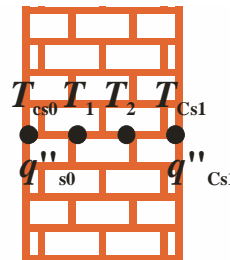


Figure 1 Illustration of variables for a single layer.

For building layers with constant thermal capacitance, the detailed governing equations have been published in Luo et al. (2008). The following

equations (7-8) are derived from the definition of the heat flux at both ends (CS0 and CS1 in Figure 1) (for details, refer to Luo et al. (2008)):

$$T_1 = -\frac{3\Delta x(2q''_{s0} + q''_{cs1})}{13.5k} + \frac{10T_{s0}}{13.5} + \frac{3.5T_{cs1}}{13.5} \quad (7)$$

$$T_2 = -\frac{3\Delta x(q''_{s0} + 2q''_{cs1})}{13.5k} + \frac{3.5T_{s0}}{13.5} + \frac{10T_{cs1}}{13.5} \quad (8)$$

Similar to the derivation of the governing equations in Luo et al. (2008), the final following governing equations can be obtained by combining Equations (7-8) with the two thermal balance equations at inner nodes 1 and 2 as shown in Figure 1:

$$\left. \begin{aligned} & \left\{ \frac{\partial(\rho_0 C p_0 T_{s0})}{\partial t} + \frac{40}{13.5} \frac{\partial(\rho_1 C p_1 T_{s0})}{\partial t} + \frac{3.5}{13.5} \frac{\partial(\rho_2 C p_2 T_{s0})}{\partial t} \right. \\ & + \frac{14}{13.5} \frac{\partial(\rho_1 C p_1 T_{cs1})}{\partial t} + \frac{10}{13.5} \frac{\partial(\rho_2 C p_2 T_{s1})}{\partial t} \\ & \left. - \frac{8L_t}{13.5k} \frac{\partial(\rho_1 C p_1 q''_{s0})}{\partial t} - \frac{L_t}{13.5k} \frac{\partial(\rho_2 C p_2 q''_{s0})}{\partial t} \right\} \\ & = \frac{1}{13.5} \left\{ -T_{s0} + T_{cs1} + \frac{L_t}{k} q''_{s0} \right\} \end{aligned} \right\} \quad (9)$$

$$\left. \begin{aligned} & \left\{ \frac{\partial(\rho_{cs1} C p_{cs1} T_{cs1})}{\partial t} + \frac{40}{13.5} \frac{\partial(\rho_2 C p_2 T_{cs1})}{\partial t} + \frac{3.5}{13.5} \frac{\partial(\rho_1 C p_1 T_{cs1})}{\partial t} \right. \\ & + \frac{14}{13.5} \frac{\partial(\rho_2 C p_2 T_{s0})}{\partial t} + \frac{10}{13.5} \frac{\partial(\rho_1 C p_1 T_{s0})}{\partial t} \\ & \left. - \frac{8L_t}{13.5k} \frac{\partial(\rho_2 C p_2 q''_{cs1})}{\partial t} - \frac{L_t}{13.5k} \frac{\partial(\rho_1 C p_1 q''_{cs1})}{\partial t} \right\} \\ & = \frac{1}{13.5} \left\{ T_{s0} - T_{cs1} + \frac{L_t}{k} q''_{cs1} \right\} \end{aligned} \right\} \quad (10)$$

For greenhouse coverings, extra heat flux from the solar radiation are added to the surface heat fluxes q''_{s0} and q''_{cs1} .

The sensitivity of the spatial step Δx on the final results has been studied in Luo et al. (2008), showing that even for 0.1m thickness of building material with two inner nodes, the relative error is less than 0.2%. As for the time step, Luo et al. (2006) showed comparison of resulting using both 600s and 3600s of time steps with analytical solutions are satisfactory.

Ground floor model

As showed in Fig. 2, the ground floor is assumed to be a "wall" comprising several layers of construction, with an air gap and 20 layers of soil each with a thickness of 0.2 m. The heat flux at the lower surface of the deepest layer is assumed zero (referring to Luo et al. (2010a)).

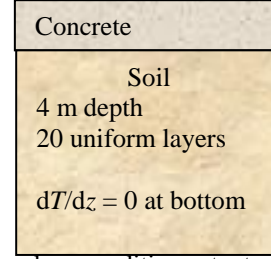


Figure 2 Boundary conditions at a typical floor.

Energy balance equations for zones

For any zone, the zone air temperature is defined as a new primitive variable. The energy balance equation applied to this zone can be obtained by the following:

$$V_r \rho_a C p_a \frac{\partial T_r}{\partial t} = \sum_{i=1}^{N_r} A_i h_{ri} (T_{ri} - T_r) + C p_a \dot{m}_{inf} (T_{env} - T_r) + \dot{q}_{in} \quad (6)$$

in which \dot{m}_{inf} is the mass flowing rate (in kg/s) of the infiltration from environments (including other zones or the atmosphere), T_{env} represents the temperature of the environmental air, V_r the volume of the zone, ρ_a , $C p_a$ and T_r represent the density, thermal capacity and the temperature of the zone air respectively, A_i , h_{ri} , and T_{ri} is the area, convective heat transfer coefficient and surface temperature of the surrounding wall i respectively, and \dot{q}_{in} (in J/s) is the energy input by HVAC equipments. If the zone is air conditioned and the zone air temperature is set by the thermostat, the \dot{q}_{in} is chosen as the primitive variable to replace the zone air temperature, leading to the energy consumption of the zone becoming the output parameter.

Modelling the heat specific capacity of a PCM

The 1D first law of thermodynamics (applied to the domain between the first and third node as illustrated in Fig. 1) reads

$$\frac{\Delta x}{3} \frac{\partial(\rho_0 h_0 + 4\rho_1 h_1 + \rho_2 h_2)}{\partial t} = -k_0 \frac{\partial T}{\partial x} \Big|_0 + k_2 \frac{\partial T}{\partial x} \Big|_2 \quad (11)$$

in which h_0 , h_1 and h_2 represents enthalpy at first to third nodes in Fig. 1. Integrating Equation (11) from time instant t to $t + \Delta t$, it reads

$$\frac{\rho \Delta x}{3} (\Delta h_0 + 4\Delta h_1 + \Delta h_2) = \frac{1}{2} \left[\left(-k_0 \frac{\partial T}{\partial x} \Big|_0 + k_2 \frac{\partial T}{\partial x} \Big|_2 \right) \Big|_t + \left(-k_0 \frac{\partial T}{\partial x} \Big|_0 + k_2 \frac{\partial T}{\partial x} \Big|_2 \right) \Big|_{t+\Delta t} \right] \quad (12)$$

$$\Delta h = \int_{T^n}^{T^{n+1}} C_p dT = C_p^{n+1} T^{n+1} - C_p^n T^n \quad (13)$$

From Equation (13), the effective specific heat capacity at the time $t + \Delta t$ (corresponding to superscript $n + 1$) can be expressed as:

$$C_p^{n+1} = C_p^n + \frac{\int_{T^n}^{T^{n+1}} C_p dT - C_p^n (T^{n+1} - T^n)}{T^{n+1}} \quad (14)$$

$$= C_p^n + \frac{\int_{T^n}^{T^{n+1}} h_{fusion} dT}{T^{n+1}}$$

It can be observed from Equation (13) that the effective specific heat capacity depends on its history and heat of fusion h_{fusion} . Therefore, governing equations (9-10) can be used for modelling the PCM materials with the thermal capacity given by Equation (14). The thermal capacity is varying with temperature.

RESULTS AND DISCUSSION

All the following results are obtained using the Modified Newcastle University Modelling and Building Energy Rating Software (Modified NUMBERS) which was developed by the authors as part of the broader investigation (refer to Luo et al. (2011), Luo et al. (2010a, b)). The weather model includes a solar radiation model which calculates the solar radiation heat flux of any inclined wall surface based on the global and diffusive solar radiation upon the horizontal plane, and a convective heat transfer coefficients (CHTC) model which calculates the CHTC of any building wall in terms of the wind speed, wind direction and the building geometry. The software provides two options for the solar radiation model: the ASHRAE simplified model (according to ASHRAE (2001)); and the Perez model (according to Perez et al. (1990)). The NUMBERS software supports four options for the CHTC model: the simple method; the ASHRAE 1993 method; the MOWITT method; and the Doe-2 method (for details, refer to Luo et al. (2006)). The major wall systems employed in the present study are double polythene films with air gap. The thermal properties for the polythene are listed in Table 1. Although the time step can be as small as seconds, all time steps in the present paper have been chosen as 1 hour. Luo et al. (2011), Luo et al. (2010a, b) provided validation of the model for the thermal performance of buildings against measurements. The validation for the phase changing materials will be tested against experiments using the phase changing materials in the greenhouse with cooperating with National Centre for Greenhouse Horticulture, NSW Department of Primary Industries, Research Road, Narara NSW 2250, Australia.

Because no reliable data about greenhouse plants are available for validating the plant submodel in the modified software, the model for the leaf surface temperature is not included in the present paper. The geometry of the model as shown in Figure 3 is assumed as 9 (length) × 6 (wide) × 3 (height) metre from the propagator house size. The grey sheets shown in Figure 3 are PCM inner walls with 1 metre high and 9 metres long. The 2003 Newcastle weather data is used in the present model.

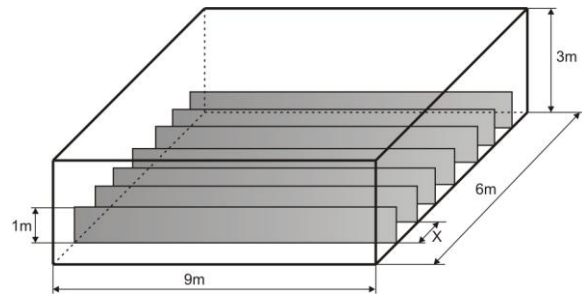


Figure 3 Configuration of the Green house with PCM inner walls. The Front is the South.

Table 1 Thermal properties for the greenhouse canopy

| Layers | Thermal capacitance (ρC_p) | Thermal conductivity (k) | Thickness | Thermal resistance |
|---------|------------------------------------|------------------------------|-----------|--------------------|
| | J/m ³ K | W/mK | m | Km ² /W |
| film | 1.4e6 | 0.2 | 0.001 | |
| Air gap | - | - | - | 0.1311 |
| film | 1.4e6 | 0.2 | 0.001 | |

Sensitivity of greenhouse inside air temperature to solar absorption coefficient of the ground surface

The ground plays very significant role in adjusting the greenhouse inside temperature. Because the ground has high thermal capacitance which is defined as the product of density and specific heat capacity, it can store heat from solar radiation at daytime and release the heat to the greenhouse during night. The ground is comprised of 20 layers of soil with 0.2 metre thickness each layer. The thermal capacitance of the soil is 1613 kJ/m³K, and the thermal conductivity is 1.205 W/mK. Shown in Figure 4 is the greenhouse inside air temperatures using floor solar absorption coefficients 0.4, 0.5 and 0.6. It is observed that higher solar absorption coefficient, higher peak temperature. Additionally, the effect of the solar absorption coefficient on the minimum night temperature is not as obvious as on the peak temperature, showing a little bit higher minimum night temperature for higher solar absorption coefficient due to the heat storage of the soil.

Sensitivity of greenhouse inside air temperature to ventilation

Ventilation of the greenhouse, characterised by the air exchange rates ach defined as the times of the greenhouse volume exchanged between inside and outside air, is caused by ventilation fan, opening cuts and/or cracks in the canopy. The present modelling greenhouse (Propagator 4) involved no heating, cooling in winter, and was operated only during harvest times by opening doors, with cooling in

summer provided with passive ventilation through open ends of the greenhouse covered with insect mesh. Therefore, it is reasonably suggested from the comparison between Figures 4 and 5 that the ach in the Propagator 4 will be higher than 1. Shown in Figure 5 is the comparison of the greenhouse inside air temperature using 1, 5 and 10 of ach with the outside air temperature. It is observed that the minimum greenhouse air temperature at night with 5 and 10 of ach is similar to the measured greenhouse temperature as shown in Figure 6, indicating that the ach in greenhouse Propagator 4 is reasonably higher than 5. In addition, the proper sealing of the greenhouse will increase the minimum temperature at night, resulting in reducing the heating load to keep the greenhouse temperature above 16-18 °C as shown in Figure 5.

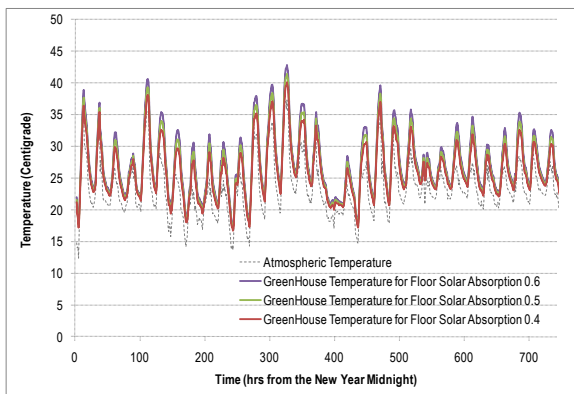


Figure 4 Comparison of the greenhouse air temperature with various floor surface solar absorption coefficients (without PCM) in summer time (January 2003).

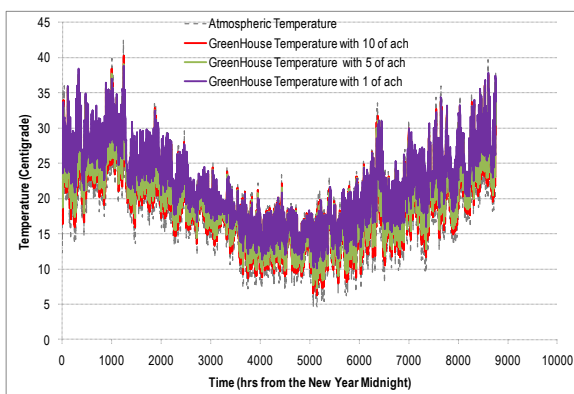


Figure 5 Comparison of the greenhouse air temperature with varying ventilation rates (ach: air exchanging rate per hour) in 2003.

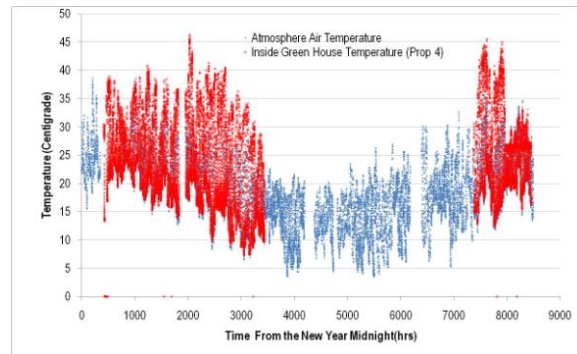


Figure 6 Comparison of the measured greenhouse air temperature with atmosphere air temperature in 2010.

Sensitivity of greenhouse inside air temperature to the thickness of the internal PCM wall

The melting point, the heat of fusion, thermal capacitance (ρC_p) and thermal conductivity for the phase changing material used in the present model are 16 °C, 150 kJ/kg, 2360 kJ/m³K, and 1.205 W/mK respectively. The total amount of PCM used is 3.96 m³ which is equivalent to 36 m² of internal PCM wall with thickness of 110 mm, or 72 m² of PCM wall with thickness of 55 mm, or 144 m² of PCM wall with thickness of 27.5 mm. Both sides of the internal PCM wall are exposed to the greenhouse air environment. Figures 7 and 8 show the comparison of the greenhouse air temperatures (for various thickness of internal PCM walls with the same amount of PCM) with the greenhouse temperature without internal PCM wall and outside air temperature. The analysis clearly indicates that the PCM significantly reduces the fluctuation of the greenhouse air temperature for winter and summer periods, highlighting that the thinner internal PCM wall (thereby the higher surface area) resulting in lower greenhouse air temperature fluctuates. Especially in winter, the greenhouse room temperature approaches the melting temperature for the greenhouse with 27.5 mm thickness of internal PCM wall. The peak temperature in the summer also decreases when using internal PCM wall, leading to the less cooling demands in the summer. As to the cost effective of the PCM used in the greenhouse, this will be addressed in the full greenhouse model in the next stage of the project.

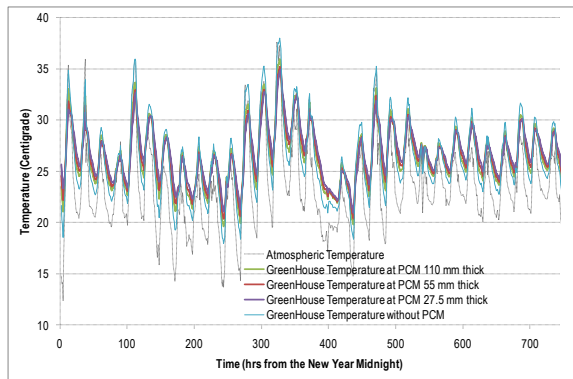


Figure 7 Comparison of the greenhouse air temperature with various thickness of same amount of PCMs in summer time (January 2003).

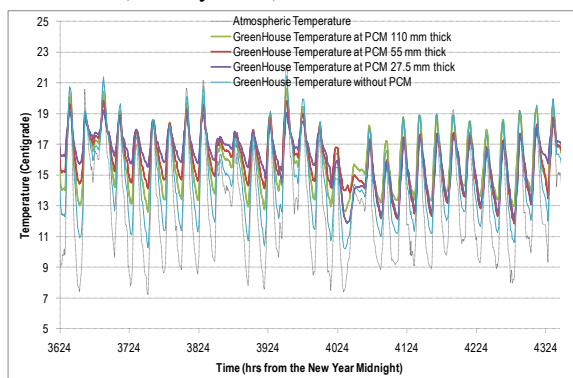


Figure 8 Comparison of the greenhouse air temperature with various thickness of same amount of PCMs in winter time (June 2003).

CONCLUSION

The Modified Newcastle University Modelling and Building Energy Rating Software (Modified NUMBERS) is employed to model the greenhouse with internal PCM walls. The preliminary predicted result showed the same varying trends for the greenhouse temperature with the measurements. The major conclusions can be summarized as the followings:

- Ground surface solar absorption coefficients affects the daytime peak temperature.
- Ventilation of the greenhouse plays significant role for the minimum night temperature, showing that sealing the greenhouse at night would reduce the heating load a lot.
- Internal PCM wall alleviates the greenhouse inside air temperature fluctuation. With the same amount of PCM, thinner the PCM internal walls, more obvious fluctuation allevating effect.

ACKNOWLEDGEMENT

This project is supported by National Centre for Greenhouse Horticulture, NSW Department of Primary Industries, Australia.

REFERENCES

- ASHRAE (2001) Handbook of fundamentals, American Society of Heating, Refrigeration and Air Conditioning Engineers, Atlanta, GA.
- Athienitis, A. K., Liu, C., Hawes, D., Banu, D. & Feldman, D. (1997) Investigation of the thermal performance of a passive solar test-room with wall latent heat storage. *Building and Environment*, 32, 405-410.
- Bransier, J. (1979) Periodic storage by latent heat on the fundamental aspects of the kinetics of transfers *International Journal of Heat and Mass Transfer*, 22, 875-883.
- Hay, J. E. & Davies, J. A. (1980) Calculations of the solar radiation on a inclined surface. IN Hay J.E., W. T. K. (Ed.) *Proc. of First Canadian Solar Radiation Data Workshop*, 59. Ministry of Supply and Services, Canada.
- Heim, D. & Clarke, J. A. (2004) Numerical modelling and thermal simulation of pcm-gypsum composites with esp-r. *Energy and Buildings*, 36, 795-805.
- Ibanez, M., Lazaro, A., Zalba, B. & Cabeza, L. F. (2005) An approach to the simulation of pcms in building applications using trnsys. *Applied Thermal Engineering*, 25, 1796-1807.
- Jayamaha, S. E. G., Wijeysondera, N. E. & Chou, S. K. (1996) Measurement of the heat transfer coefficient for walls. *Building and Environment*, 31, 399-407.
- Kumar, K. S., Jha, M. K., Tiwari, K. N. & Singh, A. (2010) Modeling and evaluation of greenhouse for floriculture in subtropics. *Energy and Buildings*, 42, 1075-1083.
- Luo, C., Moghtaderi, B., Hands, S. & Page, A. (2011) Determining the thermal capacitance, conductivity and the convective heat transfer coefficient of a brick wall by annually monitored temperatures and total heat fluxes. *Energy and Buildings*, 43, 379-385.
- Luo, C., Moghtaderi, B. & Page, A. (2010a) Effect of ground boundary and initial conditions on the thermal performance of buildings. *Applied Thermal Engineering*, 30, 2602-2609.
- Luo, C., Moghtaderi, B. & Page, A. (2010b) Modelling of wall heat transfer using modified conduction transfer function, finite volume and complex fourier analysis methods. *Energy and Buildings*, 42, 605-617.
- Luo, C., Moghtaderi, B., Sugo, H. & Page, A. (2006) The verification of finite volume based thermal performance software using analytical solutions and measurements. *IBPSA Australasia 2006 Conference*. The University of Adelaide, Adelaide, South Australia, Australia.
- Luo, C., Moghtaderi, B., Sugo, H. & Page, A. (2008) A new stable finite volume method for predicting thermal performance of a whole building. *Building and Environment*, 43, 37-43.

- Onishi, J., Soeda, H. & Mizuno, M. (2001)
Numerical study on a low energy architecture
based upon distributed heat storage system.
Renewable Energy, 22, 61-66.
- Perez, R., Ineichen, P., Seals, R. & Zelenka, A.
(1990) Making full use of the clearness index for
parameterizing hourly insolation conditions. *Solar
Energy*, 45, 111-11